SOME PARAMETERS OF PLASMA BLOB GENERATED BY CONICAL THETA PINCH

N. I. Alinovskii, A. N. Papyrin,
B. K. Pakhtusov, and A. G. Ponomarenko

Results are presented of a study of a plasma blob using various diagnostic methods. Plasma containing practically no impurities and having an electron temperature of about 30 eV was recorded in the head portion of the blob. Behind the head follows plasma with a high content of neutral gas and impurities. It is shown that the interaction of the discharge current with the chamber walls, which weakens markedly when a shorting discharge is used, has a significant influence on the formation of this part of the blob.

In order to conduct experiments on collisionless shock-wave generation, it is necessary to have a pre-plasma which is free of impurities and having a sufficiently high degree of ionization [1]. One of the most widely used plasma sources is the conical theta-pinch injector [2, 3]. The objective of the present study was to determine the parameters of the blob generated by such a source and to attempt to reduce the interaction of the plasma with the discharge chamber walls by the use of a shorting discharger.

The experiments were conducted on a UN-5 setup, which was described in detail in [4]. The parameters of the pre-plasma created by a slow inductive discharge (with period $T = 13$ μsec) at the instant of triggering of the conical coil were: charged particle density $n_i = (3\text{-}4) \cdot 10^{13}$ cm^{-3}; electron temperature $T_e = 1\text{-}5$ eV; and degree of ionization $\gtrsim 20\%$. The injector voltage $U_0 = 30$ kV; storage capacitance $C_0 = 1.2$ μF; and current period in coil $T_0 = 3.2$ μsec. The experiments were conducted with continuous working gas (hydrogen) flow into the chamber. The value of the quasistationary magnetic field H_0 varied in the range from 0 to 2 kOe.

To determine the plasma density (n_i, n_0) and temperature (T_e) the blob was probed by keV-energy neutral particle beams. The atomic and molecular hydrogen beams were obtained by ion charge exchange in the extraction electrode channel of a high-frequency ion source on the gas exhaust from the source discharge bulb. After removal in an electric field of the unrecharged ions, the beams were introduced into the plasma setup chamber. Upon passage through the plasma blob there was attenuation of the beams as a result of charge transformation of the sounding particles and deflection of the newly formed ions from the original trajectory by the transverse magnetic field of the setup.

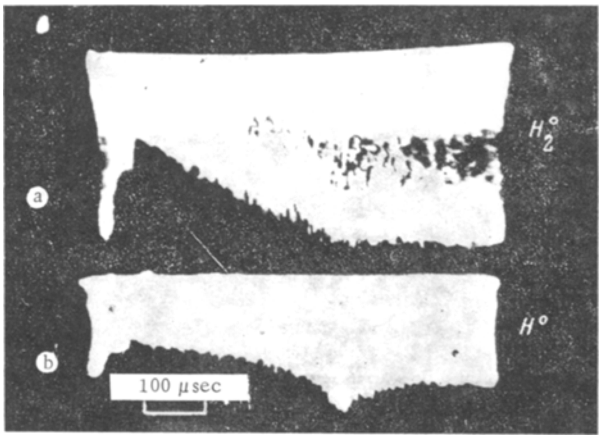

Fig. 1. Atomic and molecular hydrogen beam attenuation in plasma blob (particle energy, 4 KeV).

The attenuation of the atomic hydrogen beam was due primarily to resonant charge exchange on the plasma protons. For a beam energy of several keV and sufficiently high plasma electron temperature (more than a few tens of eV), the molecular hydrogen beam attenuation is due both to charge

Novosibirsk. Translated from Zhurnal Prikladnoi Mekhaniki i Tekhnicheskoi Fiziki, Vol. 10, No. 6, pp. 105-110, November-December, 1969. Original article submitted March 25, 1969.

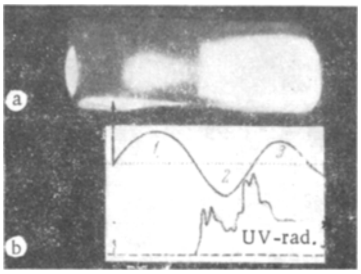

Fig. 2

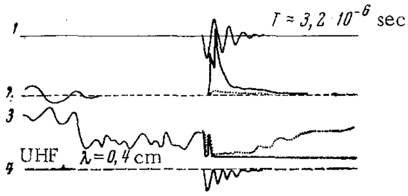

Fig. 3

Fig. 2. a) Scan photograph of plasma luminescence, made through transverse slit located 10 cm from injector; b) current in conical coil and UV radiation signal from plasma (3.2 μsec).

Fig. 3. Data from UHF transillumination ($\lambda = 4$ mm) and recordings of UV radiation from plasma in two injector operating regimes.

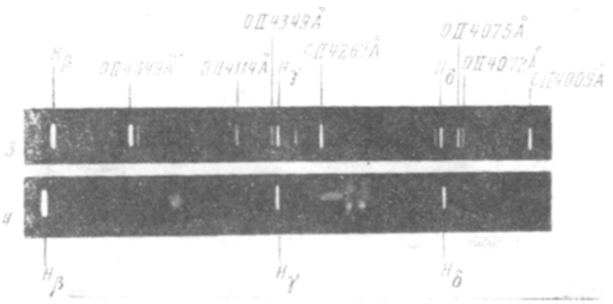

Fig. 4. Plasma spectrum obtained on ISP-51 spectrograph in the usual source operating regime and in the regime with shorting discharger.

exchange on protons and, to a marked degree, to ionization of the beam particles by the plasma electrons. For a low electron temperature and a correspondingly low degree of ionization $\alpha = n_i/(n_i + n_0)$ ($\alpha \le 0.1$), the beam attenuation will be determined both by proton charge exchange and by stripping by the plasma neutral component.

The neutral beams, attenuated as a result of interaction with the plasma blob, entered a stripping chamber, where they were partly transformed into charged beams. After passing through the energy analyzer, the H^+ and H_2^+ ions were separated in space by a magnetic mass analyzer and were recorded with the aid of an ion-electron converter on a FEU-16B photomultiplier. The output signal from the photomultiplier was modulated with a frequency up to 500 kHz applying a modulating voltage to the photocathode. The apparatus and the diagnostic technique itself are described in more detail in [5-8]. In the study we also made high-speed photographic recordings of the plasma luminescence by means of the ZIM-1 and ZIM-2 electron-optical converters in the single-frame regime with an exposure time of $\tau \approx 15$ nsec and the PIM-3 and UMI-93 electron-optical converters in the chronographic regime. An ultraviolet radiation sensor was used to record the plasma radiation in the $\lambda \le 1500$ Å region. The electron density n_e was determined by UHF transillumination of the blob at the $\lambda = 4$ mm wavelength.

The neutral particle beam probing of the blob was carried out at a distance of $l = 1$ m from the conical injector.

Figure 1 shows an oscillogram of atomic and molecular hydrogen beam attenuation as they pass through the plasma blob (particle energy, 4 keV). Analysis of this oscillogram gave the following results: duration of clearly identifiable head portion of blob, $t \approx 15$ μsec; ion density in the blob, $n_i \approx 7 \cdot 10^{13}$ cm^{-3}, $T_e \approx 30$ eV (longitudinal dimension $l_0 \approx 15$ cm). Then we note the arrival of weakly ionized plasma (ion longitudinal energies on the order of a few eV) with the following parameters at the density peak: ion density, $n_i = (1\text{-}2) \cdot 10^{14}$ cm^{-3}; neutral density $n_0 \approx 10^{15}$ cm^{-3}. Thereafter n_i decreases monotonically with decrease of the quasistationary magnetic field intensity.

Figure 2 presents the results of measurements (electron optical converter, UHF probing) performed immediately downstream of the coil (at 10 cm from the exit face). We see from the continuous scan photograph (Fig. 2a) that during the time of the first half-period for the case of parallel magnetic fields (shock coil field and quasistationary field), a blob is generated whose transverse dimension is approximately equal to half the tube diameter, and therefore the departing plasma occupies the entire chamber section. An electron-optical study of the dynamics of the processes near the injector coil [4] showed that beginning with the

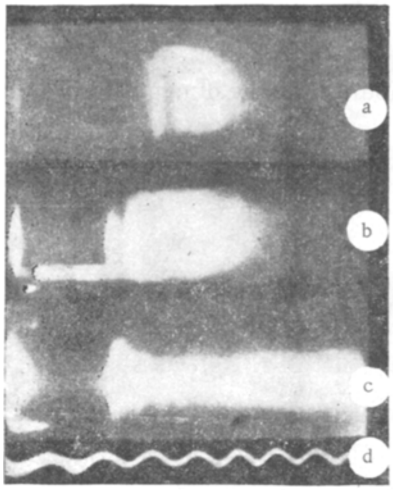

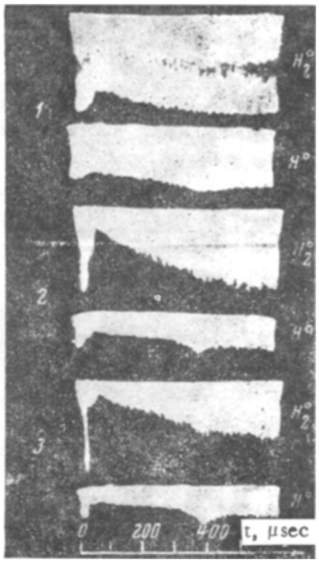

Fig. 5　　　　　Fig. 6

Fig. 5. Scan photographs of plasma radiation (transverse slit located 10 cm from coil), taken: a) in light of the O P 4649 Å line; b) in integral light; c) in integral light with shorting discharger activated; d) calibration frequency $f = 10$ MHz.

Fig. 6. Oscillograms of atomic and molecular hydrogen beam attenuation for various values of quasistationary magnetic field on plasma blob (1-H = 0, 2-H = 1 kOe, 3-H = 2 kOe.

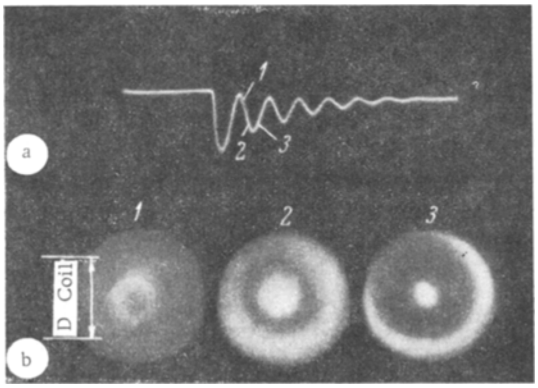

Fig. 7. a) Current in coil in regime with shorting discharger ($T/2 \approx 1.6$ μsec); b) single-frame photographs taken through chamber end wall (exposure time about 15 nsec).

second half-period, a current layer is formed which is in direct contact with the chamber wall, and from that very moment blanking out of the UHF signal was recorded ($\lambda = 4$ mm) (Fig. 3) and UV radiation from the plasma appeared (Figs. 3 and 2b). These facts indicate interaction of the wall current with the surface of the glass chamber, while apparently the absorbed working gas and oil films which vaporize during the discharge are responsible for the particle concentration increase in the plasma ejected from below the coil in the second and following half-periods.

The interaction of the discharge current with the glass surface during repeated breakdowns causes continuous and ever increasing input of neutral gas from the chamber walls, and thus the velocities of the plasma radial pinch and axial efflux decrease, although the overall scheme of the phenomena taking place near the coil remains similar to the initial half-periods of injector operation [4]. The total number of particles entering the volume during the discharge time was established with the aid of an ionization tube operating in the pulsed mode. This number was $\approx 10^{18}$. This means that the particle concentration in the plasma increased in comparison with the initial concentration by more than an order and reached a value close to 10^{15} cm^{-3}. A qualitative illustration of the presence of contaminants in the plasma is shown by the plasma spectrum (Fig. 4), in which there are doubly charged ions of oxygen and carbon. Another illustration is the scan photograph shown in Fig. 5, where we see that intense radiation of the 4649 Å oxygen ion line begins right after the first wall breakdown, and thereafter it repeats the integral radiation of the blob.

Let us estimate the surface density of the gas adsorbed on the chamber walls. We can write for the total number of particles entering the discharge ($\approx 10^{18}$):

$$2\pi R l_1 N = \pi R^2 l_2 n_0$$

Here R is the radius of the discharge chamber; l_1 is the dimension at which gas desorption takes place, approximately equal to the coil length; l_2 is the distance over which the desorbed gas propagates; N is the sorbed gas surface density; and n_0 is the density of the gas desorbed into the volume.

Hence

$$N = \frac{n_0 R}{2} \frac{l_2}{l_1}$$

For $l_2/l_1 \approx 10$, $n_0 \approx 10^{15}$ cm^{-3}, and R = 8 cm we find N $\approx 4 \cdot 10^{+16}$ cm^{-2}, which corresponds to about a hundred monolayers [9] and will obviously be a film of heavy hydrocarbons – oil cracking products from the diffusion pump [10] and the working gas itself, completely "stripped" during the discharge.

Thus, we can speak of the existence of the head part of the blob, formed during the first discharge current half-period and having the following parameters: density close to that of the pre-plasma and equal to $\sim 7 \cdot 10^{13}$ cm^{-3}, total number of particles in the head part $\sim 10^{17}$, $T_e \approx 30$ eV, temporal extent of this part of the blob at a distance $l = 1$ m from the source t = 10–15 μsec, and the second part with a large amount of neutral gas and impurities. Measurements made previously on this same setup with impulsive gas entry [11] with the aid of a charged particle energy analyzer showed that the ion and electron density profile also consists of two parts, with the value of the density in the first part having the lower magnitude. During mass spectroscopic analysis of the blob it was shown that the first part consists primarily of hydrogen, while the composition of the second part includes a considerable fraction of singly charged contaminant ions – carbon and calcium. The absence of multiply charged contaminant ions indicates a low electron temperature in this part of the blob.

Figure 6 shows oscillograms of the attenuation of neutral beams upon passage through the plasma blob for different values of the quasistationary magnetic field H_0. We see that the head part of the blob appears only in the strong magnetic field, while for small values of H_0 the blob head apparently diffuses in the transverse direction.

In order to reduce the amount of contaminants entering the discharge, we later used a "crowbar" – a controllable vacuum discharger which shorts the injector capacitance prior to the formation of the first wall breakdown. By choice of the inductance of the shorting circuit, it was possible to establish an oscillatory current regime in the injector coil and the triggering moment was selected so that the current did not change polarity (Fig. 7a).

In this regime the end-on single-frame photographs (Fig. 7a) did not show the formation of wall breakdown. With maximal voltage on the coil (in this case the current $I = \frac{1}{2} I_{max}$), the photographs showed the formation of a current shell which does not contact the wall, but is at a distance from the wall equal to $l \approx \frac{1}{3}R$ of the chamber (Fig. 7b, frame 1), which is then compressed by the growing magnetic field (frames 2, 3). The charged particle density, recorded by probing the plasma at the wavelength $\lambda = 4$ mm, corresponds to the pre-plasma density (Fig. 3), and no contaminant ion lines are seen in the plasma optical spectrum (Figs. 4, 5). On the slit scan picture of the plasma radiation with the injector operating with the shorting discharger (Fig. 5c), we see the first blob, formed in the first half-period, and the subsequent spiral-shaped plasma filament of diameter equal to half the chamber diameter. The time duration of this plasmoid is on the order of the source operating time. The experimental facts noted above indicate that in this source operating regime the amount of neutral gas and contaminants entering the plasma was reduced markedly, since the possibility of wall current layer formation was eliminated and consequently contact of the plasma with the discharge chamber walls was avoided. It should be noted that the oscillatory current regime in the coil when operating with the crowbar, in contrast with the aperiodic attenuation after the first half-period, makes it possible to obtain along with the first fast blob the subsequent plasma filament, separated from the chamber walls and having about 50% ionization.

In conclusion the authors wish to thank V. N. Luk'yanov, B. A. Yablochnikov, and V. N. Stibunov for their assistance in carrying out the experiments.

LITERATURE CITED

1. A. M. Iskol'dskii, R. Kh. Kurtmullaev, Yu. E. Nesterikhin, and A. G. Ponomarenko, "Excitation of strong collisionless shock waves in a deuterium plasma," PMTF [Journal of Applied Mechanics and Technical Physics], vol. 6, no. 6, 1965.
2. Yu. A. Kossyi, I. S. Shpigel', and E. V. Dorofeev, "Study of inductive conical plasma source," Zh. tekhn. fiz., vol. 33, no. 5, 1966.
3. Yu. S. Azovskii, I. T. Guzhovskii, Yu. P. Mazalov, V. V. Mank, B. G. Safronov, and V. A. Churaev, "Inductive conical source of plasma blobs," Zh. tekhn. fiz., vol. 38, no. 9, 1963.
4. A. M. Iskol'dskii, Yu. E. Nesterikhin, A. N. Papyrin, and A. G. Ponomarenko, "Millimicrosecond photographic recording of processes taking place in fast theta pinch," collection: Plasma Diagnostics [in Russian], no. 2, Atomizdat, Moscow, 1968.
5. N. I. Alinovskii, Yu. E. Nesterikhin, and B. K. Pakhtusov, "Plasma diagnostic setup using multi-component fast neutral particle beam," collection: Plasma Diagnostics [in Russian], no. 2, Atomizdat, Moscow, 1968.
6. N. I. Alinovskii, Yu. E. Nesterikhin, and B. K. Pakhtusov, "Average ionization sections of neutral particle beams for electrons having Maxwellian velocity distribution," Zh. tekhn. fiz., vol. 39, no. 1, 1969.
7. N. I. Alinovskii and Yu. E. Nesterikhin, "Neutral particle source," Pribory i tekhnika eksperimenta, no. 5, 1968.
8. N. I. Alinovskii and B. K. Pakhtusov, "On a scheme for modulating the output signal of a photomultiplier," Pribory i tekhnika eksperimenta, no. 5, 1968.
9. D. J. Rose and M. Clark, Plasmas and Controlled Fusion [Russian translation], Atomizdat, Moscow, 1963.
10. V. A. Simonov, B. N. Shvilkin, and G. P. Kutukov, "Obtaining pure high-temperature plasma in quasi-stationary systems. Processes leading to entry of contaminants into the plasma," Nuclear Fusion, 1962, vol. 2, pt. 1.
11. N. I. Alinovskii, "Time-of-flight mass spectrometers for plasma study," collection: Plasma Diagnostics [in Russian], no. 2, Atomizdat, Moscow, 1968.